Ultrasound in Med. & Biol., Vol. 36, No. 10, pp. 1736–1745, 2010

0301-5629/$ - see front matter

ELSEVIER

doi:10.1016/j.ultrasmedbio.2010.06.017

● *Original Contribution*

# MODELLING THE PROPAGATION OF ULTRASOUND IN THE JOINT SPACE OF A HUMAN KNEE

Derrick White,* Joseph A. Evans,* John G. Truscott,† and Robin A. Chivers‡

*Department of Medical Physics, University of Leeds, Leeds, United Kingdom; †Centre for Bone and Body Composition Research, University of Leeds, Leeds United Kingdom; and ‡Smith & Nephew Research Centre, York Science Park, Heslington, York, United Kingdom

(*Received* 26 *January* 2010; *revised* 7 *May* 2010; *in final form* 23 *June* 2010)

**Abstract—There is strong evidence to support the clinical use of low-intensity pulsed ultrasound (LIPUS) to augment fracture healing. A previous experimental study showed that ultrasound can propagate in the joint space of a single human cadaveric knee. A full experimental investigation of this propagation is not possible due to poor reproducibility, the scarcity of human cadaveric tissues and the practical difficulties in making ultrasound measurements in the knee. The aim of the present work is to investigate whether a computer simulation (Wave2000 Pro®; Cyberlogic Inc., New York, NY, USA) can give a good representation of the experimental model. The simulations provided a good agreement with the experimental data, giving some confidence in the application of this computer simulation method as a means of determining whether ultrasound can propagate through different anatomical regions where bone is present. (E-mail: hcs8dw@leeds.ac.uk)** © **2010 World Federation for Ultrasound in Medicine & Biology.**

***Key Words:*** **Ultrasound, 1.5 MHz, Low-intensity pulsed ultrasound (LIPUS), Knee, Human, Damaged cartilage, Healing, Joint space.**

## INTRODUCTION

There is strong evidence to support the clinical use of a specific ultrasound signal [1.5 MHz ultrasound pulsed at 1 kHz, 20% duty cycle, 30 mW/cm$^2$ intensity (SATA)] to augment fracture healing. The use of this low-intensity pulsed ultrasound (LIPUS) is the subject of recent reviews by Pounder and Harrison (2008) and Romanò et al. (2009). Research into the mechanism of action of the ultrasound shows that low-intensity pulsed ultrasound with a frequency of 1.5 MHz is capable of enhancing several aspects of the fracture healing process, including the endochondral phase in which repair progresses through a chondrogenic process (Probst and Spiegel 1997; Nolte et al. 2001).

Joint cartilage may become damaged through a variety of causes, such as trauma, ageing or disease. Osteoarthritis is a major cause of joint pain and frequently manifests in the knee joint. It has been estimated (Lawrence et al. 2008) that 27 million people in the United States of America over 25 years of age have some form of osteoarthritis, of which 9.25 million have osteoarthritis of the knee. It is now speculated that low-intensity pulsed ultrasound may have a positive effect on healing such damaged joint cartilage as a result of the evidence on the effects on cartilage during bone healing cited above, and evidence for the *in vitro* stimulation of chondrocytes from explanted animal cartilage (Zhang et al. 2003) and from human cartilage (Korstjens et al. 2008). Indeed, there is preclinical evidence for the effects of LIPUS on healing articular cartilage defects in rabbits (Cook et al. 2001; Jia et al. 2005). For the ultrasound signal to be able to have this effect on articular cartilage, it is supposed that ultrasound at sufficient intensity must be able to reach the cartilage. Given the confined geometry of many joints, it is by no means obvious that this will be the case. The present work takes the example of a human knee joint and attempts to show whether and under what conditions the LIPUS signal can propagate from an externally held transducer to reach the surface of the articular cartilage.

We have shown experimentally that ultrasound can propagate in the joint space of a single human cadaveric knee (White et al. 2007). However, a full experimental

Address correspondence to: Derrick White, Ph.D., Division of Medical Physics, University of Leeds, Level 10, Worsley Building, Clarendon Way, Leeds LS2 9JT. E-mail: hcs8dw@leeds.ac.uk

investigation of this propagation is not possible due to poor reproducibility, the scarcity of human cadaveric tissues and the practical difficulties in making ultrasound measurements in the knee, primarily due to lack of space for locating detectors. A previous study by White et al. (2004), which looked at ultrasound propagation in a simple Perspex knee phantom, found significant similarities between experimental results and results calculated from a simulation in two dimensions using the same geometry and the published properties of Perspex. This gave confidence that we could attempt a simulation of a human knee using the same software, though naturally the geometry and materials are considerably more complex than in that simple case. The aim of the present work is to investigate whether a computer simulation can indeed give a good representation of the experimental model and to discuss and define those parameters, which are most significant in the fit.

## MATERIALS AND METHODS

The two-dimensional propagation of acoustic waves (and hence ultrasound) in an isotropic elastic medium can be described by eqn. (1) (Kino 1987; White 2006):

$$\rho\frac{\partial^2 \boldsymbol{w}}{\partial t^2} = \left(\mu+\eta\frac{\partial}{\partial t}\right)\nabla^2\boldsymbol{w}+\left(\lambda+\mu+\xi\frac{\partial}{\partial t}+\frac{\eta}{3}\frac{\partial}{\partial t}\right)\nabla(\nabla\bullet\boldsymbol{w}) \quad (1)$$

where:

$\rho$ = material density [kgm$^{-3}$],
$\lambda$ = first Lamé constant [Pa],
$\mu$ = second Lamé constant [Pa],
$\eta$ = shear viscosity [Pa s],
$\xi$ = bulk viscosity [Pa s],
$\nabla$ = the gradient operator,
$\nabla\bullet$ = the divergence operator,
$\partial$ = the partial differential operator,
t = time [s] and **w** is a two-dimensional column vector whose components are the x and y components of displacement of the medium at the point (x,y), *i.e.*, $\mathbf{w} = [w_x(x,y,t)\ w_y(x,y,t)]^T$.

Information on the propagation of ultrasound in two dimensions in a given system can, therefore, be obtained from the solution of the above equation with boundary conditions defined by the geometry of the system and variable parameters selected to describe the various materials present.

### *Software*

There are a variety of numerical models designed to solve the above equation and, hence, to simulate ultrasound propagation through materials. Proprietary Windows-based software (Wave2000 Pro®; Cyberlogic Inc., New York, NY, USA) was used in the present work. It computes an approximate solution to the two-dimensional (2-D) elastic (acoustic) wave equation using a finite difference method (Kaufman et al. 1999; Luo et al. 1999). This software had previously been used in our study on a Perspex "knee" (White et al. 2004).

The software program allows the user to specify objects of any shape and material that are placed in the beam of ultrasound of selected parameters emanating from a defined source. It not only provides a means of visualising the ultrasound as it propagates through a given medium but also allows the user to specify one or more receivers that measure the displacement of the medium at a location or set of locations in a simulation over time. These are equivalent to the needle hydrophones, which were used in the experimental work described in the previous paper (White et al. 2007). The solution the software generates inherently accounts for longitudinal and shear propagation including mode conversions as well as the effects of refraction, diffraction, scattering and frequency-dependent viscous losses.

Wave2000Pro® permits the geometry of the system to be created by a variety of means. Simple objects such as the transducer were constructed using the geometry functions within the software. Alternatively, PC Paintbrush (PCX) files (ZSoft Corporation, Marietta, GA, USA), which have been created using a different application, can be imported directly into the software. Thus, it is possible to convert computed tomography (CT) images, for example, into PCX images and interrogate them ultrasonically using Wave2000Pro®. Further details of this procedure by which the bones were imported are given below.

### *Materials' properties*

The numerical model describes the transmission of ultrasound through several materials. The results from this depend on the properties of the materials, which have been input to the model. In this case, the materials are human body tissues and those of interest here are cortical bone and trabecular bone. The cartilage layer had been removed from the bone before the experimental work (White et al. 2007) and was, therefore, ignored as our model aims to replicate the experimental results. The experimental knee was immersed in a bath of water so the properties of water were also required. In an intact knee, the bones are surrounded by soft tissue, mostly skin, fat and synovial fluid and the ultrasonic properties of these are not so different from those of water as to make a major difference.

For convenience, the values chosen for the necessary properties of the materials were taken from the material library provided with Wave2000Pro. These values are given in Table 1 and are discussed below. As the software

Table 1. Material properties needed for the software with values used in the present work

| | Water | Cortical bone | Marrow (castor oil) |
|---|---|---|---|
| ρ ($kgm^{-3}$) | 1000 | 1850 | 942 |
| $C_L$ ($ms^{-1}$) | 1497 | 2901 | 1507 |
| $C_S$ ($ms^{-1}$) | 3.5 | 1303 | 57.7 |
| Longitudinal attenuation coefficient ($dBcm^{-1}$) | 0.0007 | 2.03 | 0.177 |
| Shear attenuation coefficient ($dBcm^{-1}$) | 153953 | 16.8 | 9450 |

All were obtained from the Material Library Wave2000® Pro ver. 2·00.

is only capable of simulating ultrasound propagation in an isotropic medium, only the two Lamé constants $\lambda$ and $\mu$ along with the material density ρ are required for a given material to be included in a simulation. The two Lamé constants can be derived from the Young modulus $E$ and Poisson's ratio $\nu$ or the longitudinal velocity $c_L$ and the shear wave velocity $c_S$ for a lossless isotropic solid (*e.g.*, Kino 1987). The two viscosities $\eta$ and $\xi$ combine to provide the total amount of viscous damping in the material.

The ultrasonic properties of water are well characterised though it is recognised that these are dependent on temperature and there may be some small variations as a result.

Cortical bone is a very variable material and the literature gives a very wide range of values, suggesting that the properties depend not only on the species but also on the specific bone and even location within that bone. Cortical bone has an anisotropic structure with the modulus along the bone axis higher than that in the transverse directions. However, cortical bone is only present in the knee joint as an outer layer over trabecular bone and the assignment of axes is by no means clear and probably varies in an unknown way with location. It was decided, therefore, to treat cortical bone in this work as isotropic with an average value of modulus and speed of sound. The wavelength of the ultrasound in cortical bone is a few millimetres, much greater than the structural elements of the bone, so it is a fair assumption to consider it as a homogeneous material (Nicholson and Bouxsein 1999).

Trabecular bone is much more difficult to characterise. It consists of anisotropic, heterogeneous open-celled framework of mineralised tissue saturated in marrow fluid. The properties of both the bone and marrow have, therefore, to be considered. As for cortical bone, a very wide range of values is quoted in the literature. The speed of ultrasound propagation again differs between different species and bones. Nicholson and Bouxsein (1999) list a number of different values for the speed of sound in trabecular bone from a number of different sources. Values range from 1447 $ms^{-1}$ to 3441 $ms^{-1}$. In the present work, the trabecular bone is considered as a mixture of cortical bone and marrow, with the two components identified by the grey scale values in the manipulated CT images of the bone shown in Figure 1. In an alternative, extreme approach, we also considered the trabecular bone to be solid cortical bone.

Marrow exists in two forms, red and yellow, and is a fluid in a living body. In a cadaveric body, it is often considered as having properties similar to those of fat (Hoffmeister et al. 2002). In contrast, El-Sariti et al. (2006) attempted to remove all marrow from a series of specimens of trabecular bone and found that there was very little difference in the bulk ultrasonic properties when the marrow was replaced by water. In the present work, we have made the common assumption that castor oil can be used as a model for marrow and used the properties for this, which are given in the Wave2000 Pro material properties library.

*Preparation of images*

CT images of the same human knee described in our previous paper (White et al. 2007) were used to generate the geometry files required for Wave2000. A Philips M × 8000D dual slice scanner (Philips Healthcare, Guildford, Surrey, UK) acquired images with a slice thickness of 1.3 mm and a table increment of 0.6 mm. The CT data were reconstructed by the scanner software to give a series of sagittal images with 1 mm spacing through the medial condyle. The five images shown in Figure 1 are sequential, going in a medial to lateral direction from left to right and covering a volume with a thickness of 4 mm. The resolution of these images was 3.045 pixels/mm.

The precise cortical margins of the medial condyle and tibial plateau were difficult to identify in these CT images because of a Venflon (Braun, Germany) needle, which was used to identify the midsagittal plane of the

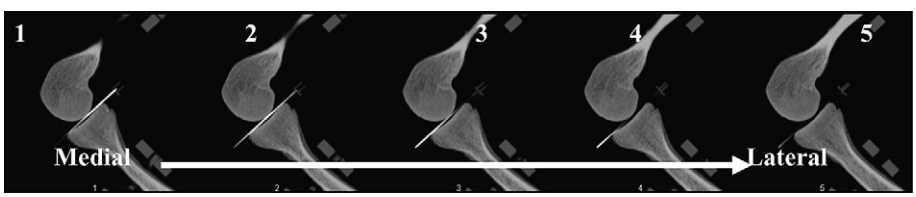


Fig. 1. Reconstructed computed tomography (CT) images of a right leg through the midsagittal plane of the medial condyle.

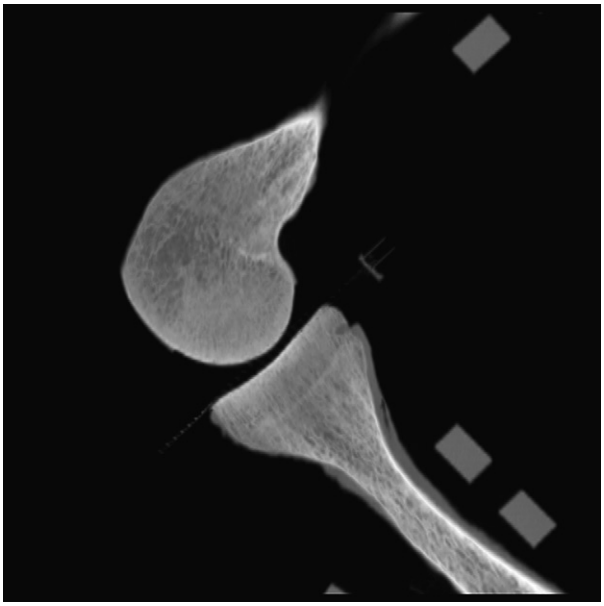

Fig. 2. Combined images of the human right knee with the Venflon needle removed.

medial condyle and that can be seen in Figure 1. The cross-section of the volume of tissue represented in Figure 1 was sufficiently uniform to allow the images 1 to 5 to be combined using ImageJ (National Institutes of Health, USA) to give Figure 2, so reducing these problems by allowing the needle to be subtracted.

Further manipulation of the image was undertaken using both ImageJ and PaintShopPro8 (Corel Corporation, Ottawa, Canada), resulting in a correctly scaled PCX file with a length of 80 mm and a width of 60 mm, a resolution of 10 pixels/mm and a colour depth of 3. By reducing the colour depth to three shades of grey, it was possible to assign the relevant material properties to these individual shades of grey: cortical bone was associated with grey level 200, marrow was associated with the grey level 100 and water was associated with the grey level 0. The material properties assigned to these are summarised in Table 1.

Axes were defined on the image of the knee for convenience and are the same as those used in our experimental work (White et al. 2007). The y-axis is along the tibia and, as the knee is flexed at about 90°, the x-axis is along the tibial plateau and approximates to the long axis of the femur. A grid was drawn using these axes and an arbitrary origin defined in the corner of the grid.

The simulation grid had a width of 80 mm (2400 grid elements) and a height of 60 mm (1800 grid elements). A grid ratio of 0.6667 was used. The finite difference grid elements had a length of 0.05 mm in both the x and y directions giving a resolution of 21 grid points per mm. The time step used in the finite difference simulation was 0.0103, which gave a total of 4872 iterations with a simulation time of 50 $\mu$s. Within the simulations, any shear waves propagating in either the marrow or

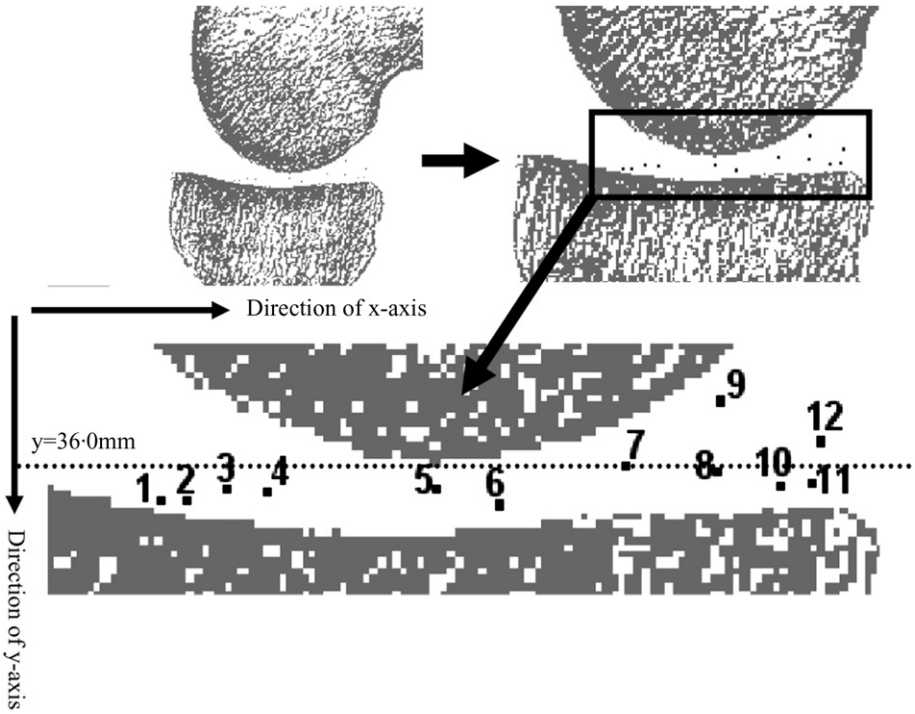


Fig. 3. Hydrophone positions obtained from plane film radiographs of the knee. The numbers identify individual hydrophone positions with "1" being the most anterior and "12" being the most posterior.

the water would be readily attenuated because of the very high shear attenuation properties of these materials (see Table1). Thus, these waves would be of no significance within the simulations and, therefore, the smallest relevant wavelength relates to the longitudinal wavelength of the 1.5 MHz ultrasound in water, which is in the region of 1 mm. The geometry files used in the simulations have a resolution of 10 pixels/mm but because the resolution of the reconstructed CT images is only 3.045 pixels/mm, the smallest geometrical detail that can be accurately represented in the simulations will be no smaller than 0.5 mm. Therefore, the accuracy of the simulation grid was deemed to be at an acceptable level to ensure stability and accuracy of the resulting simulations.

The 0.2 mm active element needle hydrophone used by White et al. (2007) was replicated in the simulations by a 0.2 mm receiver, which was configured in Wave 2000Pro® to have a uniform apodization factor and measured pressure; the default settings for gain, blanking and duration were used. The positions of these receivers in the simulation model were chosen to reproduce those of the hydrophone used experimentally. These are shown in Figure 3 for the centre of the joint. The midline of the joint is marked on the figure. This is the line where y = 36 mm, referred to an arbitrary origin.

*Simulations*

The simulations were devised to match the experimental set-up adopted by White et al. (2007) as closely as possible. In the simulations, as in the experiment, the knee was held rigidly flexed by 90° and the ultrasound source was placed 19.3 mm from the medial condyle (see Fig. 4). A total of 19 separate simulations were run, each simulating a 2 mm increment in y-coordinate of the ultrasound source transducer as used in the water tank. The 2 mm increments correspond to movements of the source in a superior/inferior direction relative to the flexed knee. For the simulations, the ultrasound transducer was modelled as a 22 mm line source with a "void backing" and a uniform apodization factor. As for the experimental runs, the source produced a 1.5 MHz sine pulse for 8 $\mu$s with zero time delay. A LIPUS pulse has a duration of 200 $\mu$s. However, pulses of this duration create spurious capacitative signals in the hydrophone, which obscure the ultrasound signals in the joint space. By keeping a pulse length of 8 $\mu$s, a close approximation to monochromacity was found that was well matched to the typical LIPUS ultrasound signal (White et al. 2006). Also, a pulse length of 200 $\mu$s would take many times longer to run in the simulations.

The 19 simulations were run a total of six times with variations to each model. The differences between each model are given below along with their respective code:

(1) The initial simulations were as those described above (I = initial simulation).
(2) All the viscous losses were removed from each of the 19 simulations (NVL = no viscous losses).

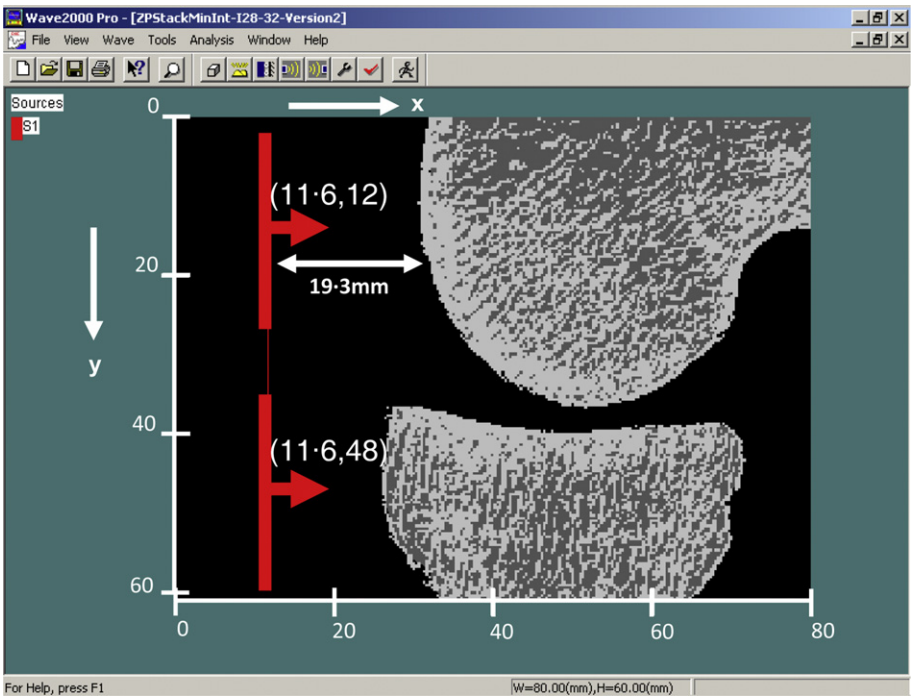


Fig. 4. Representation of Wave2000®Pro simulation model. Positions for the centre of the 22 mm ultrasound source ranged from (11.6, 12) on the simulation grid to (11.6, 48).

(3) The trabecular bone structure (bone and marrow) was replaced by solid cortical bone (NT = no trabeculae).
(4) The joint space was increased by 1mm by translating the medial condyle −0.5 mm in the direction of the y-axis and the tibia +0.5 mm in the direction of the y-axis (P1 = plus 1 mm).
(5) The joint space was increased by 2 mm by translating the medial condyle −1.0 mm in the direction of the y-axis and the tibia +1.0 mm in the direction of the y-axis (P2 = plus 2 mm).
(6) The joint space was increased by 3mm by translating the medial condyle −1.5 mm in the direction of the y-axis and the tibia +1.5 mm in the direction of the y-axis (P3 = plus 3 mm).

## RESULTS

Figure 5 shows the simulated 1.5 MHz ultrasound pulse at four time points as it propagates through the knee joint. At t = 40 $\mu$s, the ultrasound pulse is seen beginning to leave the posterior region of the joint space with reduced amplitude. A feature within Wave2000 Pro® has been used to enhance the contrast of the displayed simulation; in fact the pulse at t = 40$\mu$s has much smaller amplitude relative to the initial pulse than is suggested by the relative brightness of the images.

All lines drawn on the graphs shown in Figures 6 to 9 are purely to help locate the points plotted and have no physical meaning. The normalised readings for the experimental results with the hydrophone in position 1 and the simulated results with the receiver in positions 1 to 12 are shown in Figure 6. The graphs in Figure 6 suggest that there is a 24 mm window in the superior/inferior direction in which to place the centre of the 22 mm diameter planar ultrasound source so that the ultrasound penetrates the joint. Outside this, the intensity of ultrasound within the joint falls away rapidly. This 24 mm window corresponds to a y coordinate for the centre of the ultrasound source of between 20 and 44 mm.

It can be seen from Figure 7 that the ultrasound pressure decreases in an anterior-posterior direction for both

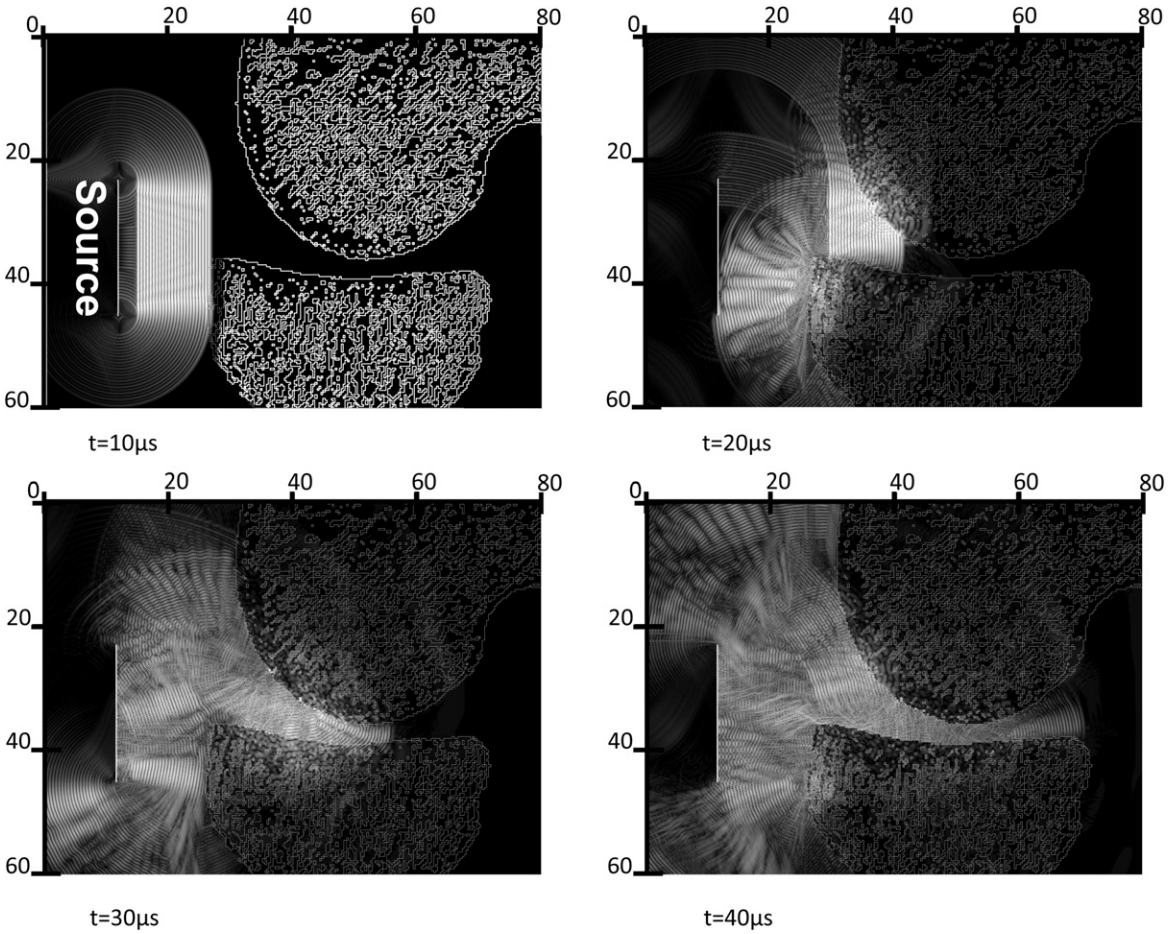


Fig. 5. Simulated 8 $\mu$s ultrasound pulse at t = 10 $\mu$s, 20 $\mu$s, 30 $\mu$s and 40$\mu$s. The pulse generation started at t = 0. Ultrasound source centre at x = 11.6 mm, y = 36 mm. The white bar is the source transducer.

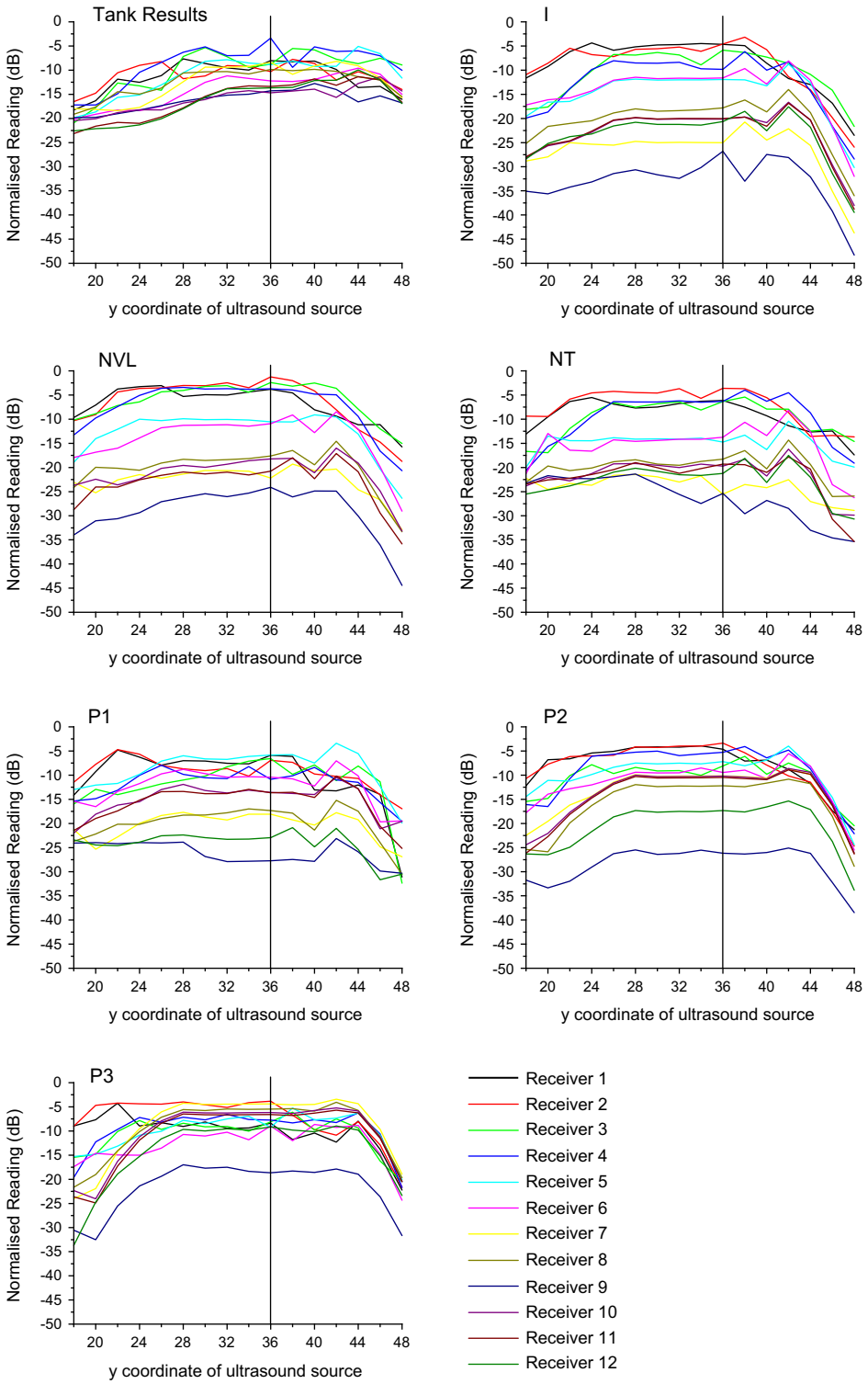


Fig. 6. Normalised hydrophone readings and receiver readings for simulations I, NVL, NT, P1, P2 and P3.

the experimental results and the six simulations. By comparison, however, the decrease is more marked with simulations 1 (I), 2 (NVL) and 3 (NT). This is perhaps more clearly shown in Figure 8 in which the differences between the experimental results and the simulations 1 (I), 2 (NVL) and 3 (NT) are seen to tend to increase in an anterior-posterior direction. Figure 8 shows that for all 12 receiver positions, simulation 6 (P3) matches

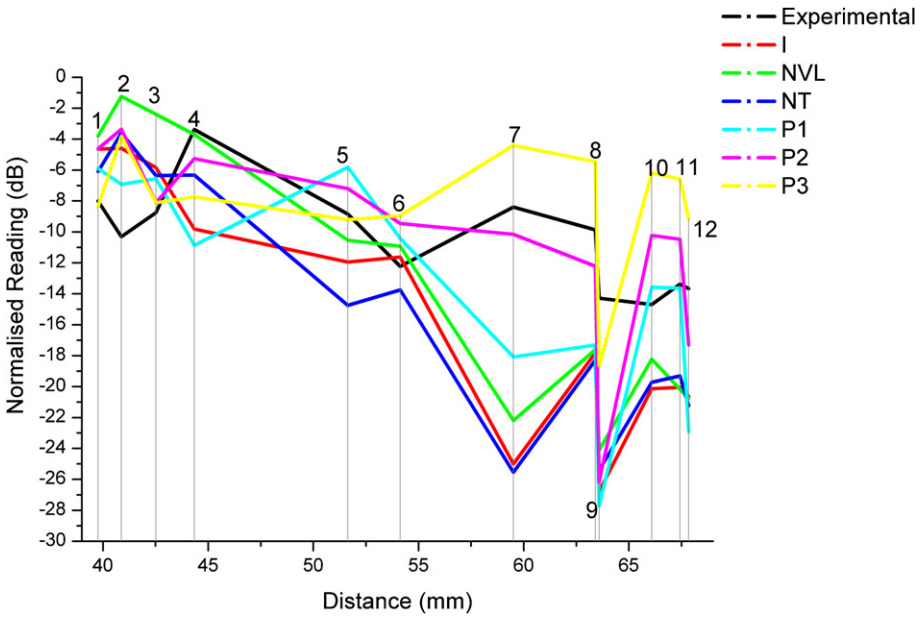


Fig. 7. Normalized mean hydrophone readings in dB for the cadaver knee plotted with the mean normalized receiver readings in dB for each of the six simulations. The 12 hydrophone/receiver positions have been identified. All readings taken with the ultrasound source centralised over the joint centre (y = 36.0 mm).

the experimental results more closely than any of the other five simulations. Interestingly, there is a sudden drop in ultrasound pressure moving from hydrophone/receiver position 8 to 9, which, according to White et al. (2007), is caused by an ultrasound shadow cast immediately behind the medial condyle. Although this is seen in both the experimental results and the simulation results, this is the region where we see the greatest difference between the experimental results and those from each simulation.

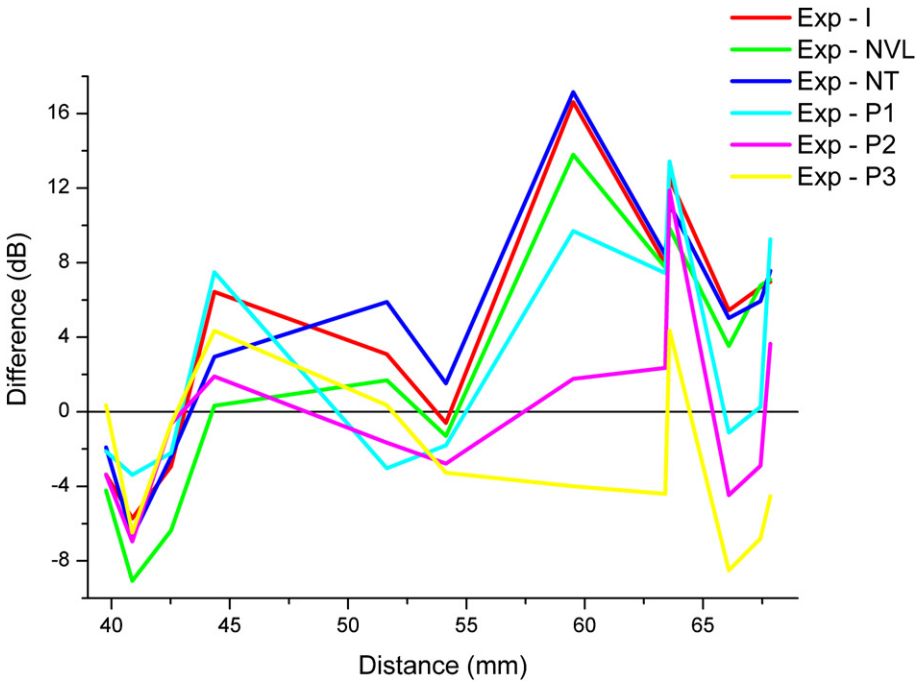


Fig. 8. Difference between the normalized hydrophone readings (experimental results) and the normalized simulation readings for the cadaver knee in dB. The 12 hydrophone/receiver positions have been identified. All readings taken with the ultrasound source centralized over the joint center (y = 36.0 mm).

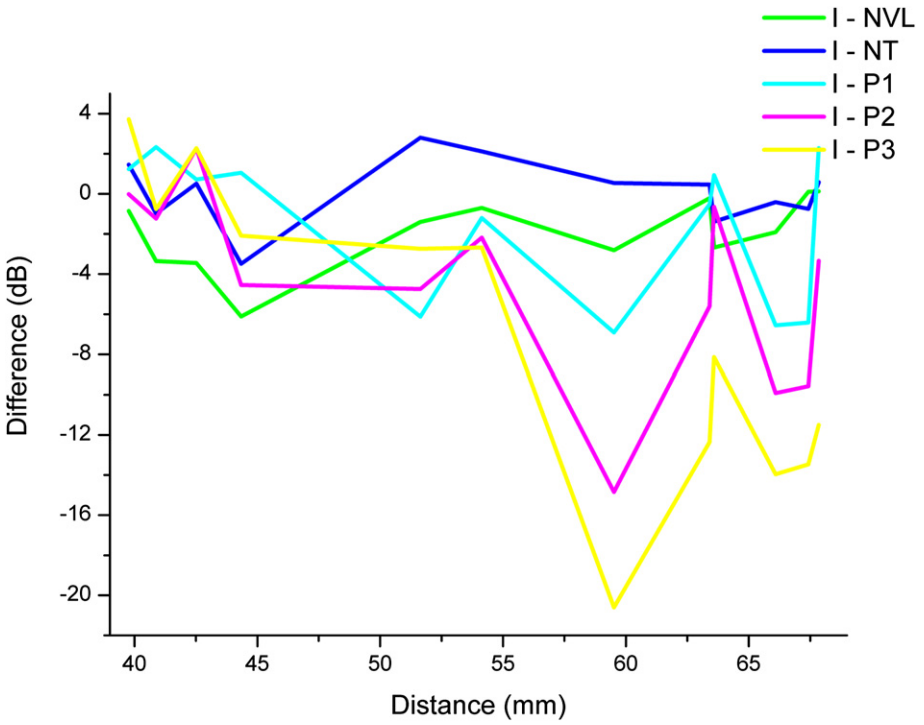


Fig. 9. Difference between the normalized simulation 1 readings and the normalized simulation readings for each of the other simulations in dB. The 12 hydrophone/receiver positions have been identified. All readings taken with the ultrasound source centralized over the joint center (y = 36.0 mm).

## DISCUSSION AND SUMMARY

It is clear that the simulations provided a good agreement with the experimental data in this specific model of ultrasound propagation through a flexed cadaveric human knee joint. Some slight differences can be noticed, though, for instance the window for placing the centre of transducer would seem to be about 24 mm (joint centre line ±12 mm) from the simulations whereas it was measured to be 28 mm (joint centre line ±14 mm) in the experimental results (White et al. 2007). This is only a small difference, will depend on the necessary signal intensity for therapeutic effects and would scarcely be noticed in the clinic.

It may be inferred that this gives some confidence in the application of this computer simulation method as a means of determining whether ultrasound can propagate through different anatomical regions in which bone is present.

Figures 7 to 9 show that when viscous losses are removed from simulation 2 (NVL) the greatest differences in the normalised receiver readings are seen in the anterior regions of the knee. However, in the posterior regions of the joint the mean normalized receiver readings are very similar for models simulation 1 (I), simulation 2 (NVL) and simulation 3 (NT), suggesting that the majority of ultrasound attenuation in this instance may be due to the geometry of the bone surfaces. The inclusion of trabecular bone in the model (simulation 1 vs. simulation 2) appears to have little effect on the ultrasound pressure in the joint space. Although this may because the trabecular bone model used was inadequate, it also offers the possibility of reducing the complexity of the simulation model by not having to create detailed models of trabecular bone and is worthy of further investigation.

The results presented in Figures 7 to 9 show that changes to the geometry of the joint space had the greatest effect on the results (simulations 4, 5 and 6). This is to be expected because the dimensions of the joint space under investigation are close to the wavelength of the incident ultrasound pulse and therefore any differences, even slight, can have a major effect. A consequence of this for further modelling in other anatomic regions is that, as dimensional accuracy is so significant, great emphasis must be placed on ensuring the accuracy of the CT (or other) images used to generate the geometry files.

A limitation of this work may be the necessity of working in only two dimensions through lack of computer resources to tackle the size of simulation grid needed in three dimensions. However, to a first approximation, this may not be as severe a limitation as it would seem. Figure 1 shows that the cross-section of the medial condyle of the knee is uniform over a width of at least

4 mm, so that there is little out-of plane geometry variation to concern the model. The ultrasound beam from a transducer of the size used at this frequency gives a uniform beam in a forward direction in water over a large part of its area at the distances considered. This shows that, in this case at least, 2-D simulations of ultrasonic propagation can be very useful in understanding a three-dimensional (3-D) problem. A 3-D version of the software is now available, but, in this geometry, it is not certain that it would provide very different results in the solution of this problem.

Based on the work undertaken here on the knee, with a relatively simple geometry, we believe that simulations of ultrasonic propagation in other anatomical sites can (even in 2-D) provide useful information that could be used to direct experimental work or inform clinical decision making about transducer placement. Clearly, this work is limited and should not be used to predict the intensities of therapeutic ultrasound in patients.

*Acknowledgments*—This project was supported by an EPSRC CASE award with support from Smith & Nephew.

## REFERENCES

Cook SD, Salkeld SL, Poptich-Patron LS, Ryaby JP, Jones DG, Barrack RL. Improved cartilage repair after treatment with low-intensity pulsed ultrasound. Clin Orthop Relat Res 2001;391: S231−S243.

El-Sariti AA, Evans JA, Truscott JG. The temperature dependence of the speed of sound in bovine bone marrow at 750 kHz. Ultrasound Med Biol 2006;32:985−989.

Hoffmeister BK, Auwarter JA, Rho JY. Effect of marrow on the high frequency ultrasonic properties of cancellous bone. Phys Med Biol 2002;47:3419−3427.

Jia XL, Chen WZ. Effects of low-intensity pulsed ultrasound in repairing injured articular cartilage. Chin J Traumatol 2005;8:175−178.

Kaufman JJ, Luo G, Bianco B, Chiabrera A, Siffert RS. Computational methods for NDT. SPIE 1999;3585:173−181.

Kino GS. Acoustic waves: Devices, imaging and analog signal processing. Chapter 2. Englewood Cliffs, NJ: Prentice Hall; 1987.

Korstjens CM, van der Rijt RHH, Albers GH, Semeins CM, Klein-Nulend J. Low-intensity pulsed ultrasound affects human articular chondrocytes *in vitro*. Med Biol Eng Comput 2008;46: 1263−1270.

Lawrence RC, Felson DT, Helmick CG, Arnold LM, Choi H, Deyo RA, Gabriel S, Hirsch R, Hochberg MC, Hunder GG, Jordan JM, Katz JN, Kramers HM, Wolfe F. Estimates of the prevalence of arthritis and other rheumatic conditions in the United States. Part II. Arthritis Rheum 2008;58:26−35.

Luo G, Kaufman JJ, Chiabrera A, Bianco B, Kinney JH, Haupt D, Ryaby JT, Siffert RS. Computational methods for ultrasonic bone assessment. Ultrasound Med Biol 1999;25:823−830.

Nolte PA, Klein-Nulend J, Albers GHR, Marti RK, Semeins CM, Goei SW, Burger EH. Low-intensity ultrasound stimulates endochondral ossification *in vitro* J Orthopaed Res 2001;19:301−307.

Nicholson PHF, Bouxsein ML. Chapters 11: Ultrasonic studies of cortical bone in vitro and 12: Ultrasonic studies of cancellous bone in vitro In: Njeh CF, Hans D, Fuerst T, Gluer C-C, Genant HK, (eds). Quantitative ultrasound assessment of osteoporosis and bone status. London: Martin Dunitz; 1999.

Pounder NM, Harrison AJ. Low-intensity pulsed ultrasound for fracture healing: A review of the clinical evidence and the associated biological mechanism of action. Ultrasonics 2008;48: 330−338.

Probst A, Spiegel H-U. Cellular mechanisms of bone repair. J Invest Surg 1997;10:77−86.

Romanò CL, Romanò D, Logoluso N. Low-intensity pulsed ultrasound for the treatment of bone delayed union or nonunion: A review. Ultrasound Med Biol 2009;35:526−529.

White D. Modelling the propagation of ultrasound in the knee. PhD Thesis, University of Leeds, 2006.

White D, Evans JA, Truscott JG, Chivers RA. Simulation of ultrasound in the knee. J Phy Conf Ser 2004;1231−1236.

White D, Evans JA, Truscott JG, Chivers RA. Can ultrasound propagate in the joint space of a human knee? Ultrasound Med Biol 2007;33: 1104−1111.

Zhang Z-J, Huckle J, Francomano CA, Spencer RGS. The effects of pulsed low-intensity ultrasound on chondrocyte viability, proliferation, gene expression and matrix production. Ultrasound Med Biol 2003;29:1645−1651.